Picosecond and Nanosecond Spectroscopies of the Photochemical Cycles of Acidified Bacteriorhodopsin†

Hiroyuki Ohtani,‡ Takayoshi Kobayashi,* and Jun-ichi Iwai

Department of Physics, Faculty of Science, The University of Tokyo, Hongo, Bunkyo-ku, Tokyo 113, Japan

Akira Ikegami

Institute of Physical and Chemical Research, Hirosawa, Wako-shi, Saitama 351, Japan

Received March 7, 1985; Revised Manuscript Received January 24, 1986

ABSTRACT: Photochemical cycles of acidified bacteriorhodopsin (bR_{605}) at 21 ± 1 °C were studied by picosecond and nanosecond spectroscopies. The sample solution "bR_{605}" was a mixture of all-trans (57%) and 13-cis (40%) components of bR_{605} ($bR_{605}^{all\text{-}tr}$ and $bR_{605}^{13\text{-}cis}$, respectively) and a small amount of bR_{568} (3%). Predominant excitation of $bR_{605}^{all\text{-}tr}$ was achieved with the use of 630-nm light. The time constant for the formation of an acidic form of the K intermediate (K_{acid}) was found to be shorter than 30 ps. The lower limit of the time constant was estimated at 2 ps. The quantum yield for the formation of K_{acid} was shown to be 0.09 ± 0.01, which is smaller than the yield of KL (0.30 ± 0.03) in a suspension at neutral pH. The absorption spectra of $bR_{605}^{all\text{-}tr}$, $bR_{605}^{13\text{-}cis}$, K_{acid}, and an acidic form of L (L_{acid}) were obtained from nanosecond time-resolved difference spectra measured with several excitation wavelengths (630, 532, and 266 nm). The time constant for the $K_{acid} \rightarrow L_{acid}$ conversion process in the acidified sample (1.5 ± 0.3 μs) is nearly equal to that for the KL → L conversion at neutral pH (1.3 ± 0.3 μs). On the other hand, the time constant for the $L_{acid} \rightarrow M$ process is much longer at low pH than at neutral pH. Difference absorption spectra between $bR_{605}^{13\text{-}cis}$ and the relevant photoproducts at low pH resemble those at neutral pH.

Photochemical cycles of bacteriorhodopsin (bR) have been extensively studied on aspects of the light-driven proton pump and of analogous visual processes (Honig, 1978; Stoeckenius et al., 1979). Three intermediates, K, L, and M, have been established in the photochemical cycle of a light-adapted purple membrane in *Halobacterium halobium* by low-temperature spectrophotometry and time-resolved spectroscopy at physiological temperatures (Kung et al., 1975; Lozier et al., 1975; Iwasa et al., 1980). Precursors of K have also been reported (Kaufmann et al., 1976; Applebury et al., 1978; Ippen et al., 1978; Matveetz et al., 1985; Nuss et al., 1985). Intermediates in the photochemical cycle of a dark-adapted purple membrane (^{610}C or Batho-bR^{13}) were found in both room temperature and low-temperature experiments (Dencher et al., 1976; Sperling et al., 1977; Kalisky et al., 1977; Iwasa et al., 1981).

The purple membrane is converted to a "blue" membrane at low pH (Oesterhelt & Stoeckenius, 1971). The blue color of the membrane is due to an acidified bacteriorhodopsin, bR_{605}, which has an absorption maximum at 605 nm (pH 2.5). It has been shown that the blue sample "bR_{605}" is a mixture of bacteriorhodopsins with *all-trans*- and 13-*cis*-retinals (60:40) (Mowery et al., 1979; Maeda et al., 1980; Smith et al., 1985) and that the sample contains a small amount of neutral form bR_{568}. It was shown that the photochemical cycles of bR_{605} in low-pH suspension and those of bR_{568} in neutral-pH suspension are different from each other by a laser photolysis study (Mowery et al., 1979). Because of the low time resolution of the experimental system used in the study, primary processes within 80 μs could not be investigated (Mowery et al., 1979). The results showed that the transient spectra depend on the excitation wavelength and that the kinetics were complicated because of the coexistence of bR_{568} and bR_{605} and intermediates in each photocycle. It is also known that 9-cis (Maeda et al., 1980; Fischer et al., 1981) and 11-cis isomers (Maeda et al., 1980) are formed by continuous irradiation with >610-nm light at temperatures between 0 and 25 °C.

In a preceding paper, we reported on the results of picosecond and nanosecond laser photolyses of bR_{605} at room temperature (Kobayashi et al., 1983). We used a 630-nm pulsed laser for selective excitation of the "bR_{605}" sample, which inevitably contained a small amount of bR_{568}. Three transient species, i.e., a precursor of an acidic form of K, the acidic form of K (K_{acid}), and an acidic form of L (L_{acid}) were observed, and it was confirmed that the conversion from L_{acid} to M was blocked. In this paper we describe the effect of pH on the time constants for these conversion processes and the quantum yield for the formation of K_{acid}. We obtained also the absorption spectra of bR_{605} with *all-trans*- and 13-*cis*-retinals (abbreviated hereafter to $bR_{605}^{all\text{-}tr}$ and $bR_{605}^{13\text{-}cis}$, respectively) and of the photochemical products of $bR_{605}^{13\text{-}cis}$ by calculation using the observed transient difference spectra.

Materials and Methods

Materials. Purple membrane fragments of *H. halobium* R_1M_1 were purified according to the process described by Oesterhelt and Stoeckenius (1974). The acidic form of purple membrane "bR_{605}" was prepared by the deionization of purple membranes. Membrane suspensions (absorbance at 560 nm = 0.8–1.2, 2-mm light path length) were deionized on a cation-exchange column of 20-mm diameter and 80-mm length (acidic form of Dowex 50W) at room temperature. The

† This work was partly reported in Kobayashi et al. (1984a,b) and Ohtani et al. (1984). This work was supported in part by the following grants: a Grant-in-Aid for Special Distinguished Research (60115004) from the Ministry of Education, Science, and Culture, grants from Toray Science and Technology Foundation and Kurata Science Foundation to T.K., and Special Coordination Funds for the Promotion of Science and Technology from the Agency of Science and Technology of Japan to A.I.

‡ Present address: Hamamatsu Photonics K.K., Ichino-cho, Hamamatsu-shi, Shizuoka 435, Japan.

0006-2960/86/0425-3356$01.50/0

suspensions were washed with distilled water several times just before the deionization treatment. The resin was alternately treated with 1 N NaOH and 1 N HCl 3 times and then washed with distilled water until the pH of water-washed supernatant became neutral. The deionized suspensions were kept in plastic tubes to avoid contact with glass. The suspensions of "bR_{605}" thus obtained were transparent and stable enough for stationary and transient absorption measurements. The absorption maximum (605 nm) of the sample agreed well with that of the acidified purple membrane in polyacrylamide gel at pH 2.0 (Mowery et al., 1979), while the pH of the sample was measured to be 5.5 with a pH meter. Therefore, the absorption maximum is not dependent on the pH of the bulk solution but on the local pH near the membrane surfaces (Kimura et al., 1984).

Molar Extinction Coefficient of "bR_{605}". A sample solution of "bR_{605}" (I) was converted to a neutral pH solution (II) by the addition of aqueous sodium hydroxide. Solution II was light-adapted with a tungsten lamp until the absorption maximum shifted to 568 nm. The molar extinction coefficient of "bR_{605}" (a mixture of chromoproteins with *all-trans*-retinal and those with 13-*cis*-retinal) was obtained by using the absorbances of the regenerated bR_{568} ($\epsilon_{max} = 6.27 \times 10^4$ mol^{-1} dm^3 cm^{-1}; Rehorek & Heyn, 1979) and sample solution I.

Laser Photolysis. The light source for picosecond spectroscopy was a passively mode-locked (Kodak 9740 dye in chlorobenzene as a saturable absorber) Nd:YAG laser (1064 nm, Quantel, YG472). The second harmonic of the laser was focused into an acetone cell to stimulate the first Stokes of the Raman scattered light by acetone [630 nm, 20-ps full width at half maximum (fwhm), 76-90 μJ; Iwai et al., 1984], which was used for the excitation of samples. From the intensity and absorption cross section it was estimated that 73 ± 7% of the bR_{605} molecules were excited in the irradiated area of 2 mm^2. A picosecond continuum was generated by focusing the fundamental light into a D_2O cell and was divided into two beams with nearly equal intensity, one of which was used for a probe and the other for a reference. The probe light, with pulse energy slightly less than 10 nJ, was focused on an area slightly less than 0.2 mm^2 at the center of the excited region. The path length of the probe light was 2 mm in the sample. The probe and reference lights were separately detected by two multichannel photodiode arrays (MCPD, 512 channels, Union Giken) coupled with a grating polychromator (Union Giken, f = 20 cm, 600 grooves/mm). The output signals of the MCPD's were transferred to a microcomputer (NEC, PC8001)–minicomputer (DEC, MINC 11) analyzing system. Details of the experimental system for the measurement of picosecond time-resolved absorption spectra were described elsewhere (Iwai et al., 1984).

The time dependence of absorbance change of bR_{568} was measured with the use of the picosecond spectroscopy apparatus for time standardization of the delay time (±5 ps). Twelve to sixteen pairs of excitation and nonexcitation data were averaged and used for the calculation of the transient spectra.

Excitation light sources for nanosecond spectroscopy were the fourth (266 nm, 5-ns fwhm, 0.5 mJ) and second (532 nm, 5-ns fwhm, 0.5 mJ) harmonics of a *Q*-switched Nd:YAG laser (Quanta-Ray, DCR-1A) and the first Stokes Raman scattering of 532-nm light by acetone (630 nm, 5-ns fwhm, 90 μJ). The excitation light pulses were focused on an area of 4 mm^2. A probe light source was a xenon flash lamp (300 W, 500 μs, Varian Xenon Illuminator VIX 300F). The path length of the probe light was 3 mm in the sample. Output signals of a photomultiplier (Hamamatsu Photonics, R666S or 1P28) coupled with either a Shimadzu Bausch & Lomb monochromator (f = 17 cm, 1350 grooves/mm of grating) or a Ritsu MC10N monochromator (f = 10 cm, 600 grooves/mm of grating) were digitized by a transient recorder (Iwatsu, DM901) and averaged with a microcomputer (NEC, PC8001). Details have been described elsewhere (Iwai et al., 1984).

All measurements were performed at 21 ± 1 °C. Samples were stirred after one or two laser shots to avoid photochemical and/or thermal damages.

Table I: Molar Fractions of $bR_{605}^{all\text{-}tr}$, $bR_{605}^{13\text{-}cis}$, and bR_{568} in the Sample and Fractions of Photon Number Absorbed by the Three Components out of the Total Absorbed Photon Number

	$bR_{605}^{all\text{-}tr}$	$bR_{605}^{13\text{-}cis}$	bR_{568}
f_i[a]	0.57	0.40	0.03
F_i(630 nm)[b]	0.77 ± 0.07	0.22 ± 0.07	0.01
F_i(532 nm)[b]	0.45 ± 0.02	0.50 ± 0.02	0.05
F_i(266 nm)[b]	0.57	0.40	0.03

[a] Molar fractions for $bR_{605}^{all\text{-}tr}$, $bR_{605}^{13\text{-}cis}$, and bR_{568} are denoted by f_i's (i = T, C, and P, respectively). [b] Fractions of photon number absorbed by component i were calculated by $F_i(\lambda) = f_i\epsilon^i(\lambda)/[f_T\epsilon^T(\lambda) + f_C\epsilon^C(\lambda) + f_P\epsilon^P(\lambda)]$.

Results

The sample solution "bR_{605}" contains $bR_{605}^{all\text{-}tr}$, $bR_{605}^{13\text{-}cis}$, and a small amount of bR_{568}. The molar fraction of $bR_{605}^{13\text{-}cis}$ in "bR_{605}" is 0.4 (Mowery et al., 1979; Maeda et al., 1980; Smith et al., 1985). These values were obtained by the method described in the Appendix. The fraction of bR_{568} (f_P) in "bR_{605}" was determined to be 0.03 from the concentration of KL intermediate (Shichida et al., 1983) formed by a 532-nm excitation pulse. Table I shows the molar fractions of the components in "bR_{605}" and fractions of photon number absorbed by the components out of the total number of absorbed photons. The fractions of the three components excited depend on the excitation wavelength. Intermediates in the three photocycles were distinguished from each other by the analysis of the excitation-wavelength dependence of the transient spectra and the temporal behaviors.

Picosecond Time-Resolved Spectroscopy with 630-nm Excitation Light. Figure 1 shows the time-resolved difference spectra following 630-nm excitation of the "bR_{605}" sample. Of the three components in bR_{605}, mainly $bR_{605}^{all\text{-}tr}$ is excited by the 630-nm light. The highly sensitive detection system enabled us to use excitation light sources with low pulse energy (76–90 μJ). The intensities of the scattered excitation light pulses were smaller than those of probe pulses. The spikes at 630 nm shown in Figure 1 are due to the scattered excitation light pulse, the intensity of which fluctuates from shot to shot. Negative and positive absorbance changes appear in the 550–680- and 500–520-nm regions, respectively, 21 ps after excitation (Figure 1d). All the spectra between 43 and 217 ps (Figure 1f–i) resemble that at 100 ns (Kobayashi et al., 1983). The increase in absorbance at longer wavelengths observed at 43 ps is due to the formation of the K intermediate in the acidic form (K_{acid}). We could not detect small spectral changes due to the S (or J) → K (Applebury et al., 1978; Matveetz et al., 1985) and K → KL (Shichida et al., 1983) conversions, which had been observed in the photocycle of bacteriorhodopsin in neutral pH suspension.

Parts a and b of Figure 2 show the time dependencies of the absorbance changes averaged over the 570–620- and 640–690-nm spectral regions, respectively. Curves 1, 2, 3, and 4 are the best fitted convolution curves obtained for exponential

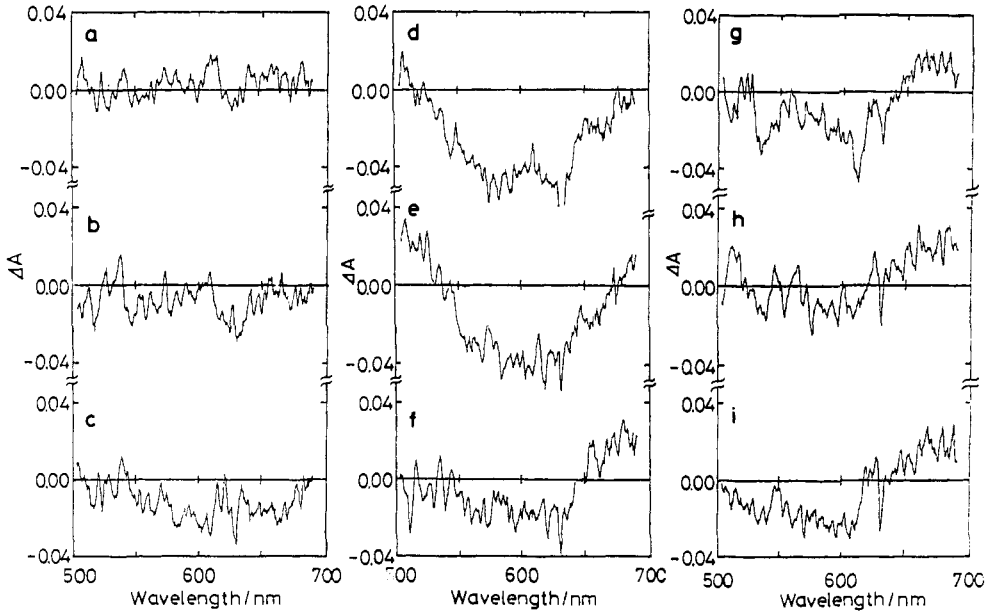

FIGURE 1: Picosecond time-resolved difference spectra following 630-nm excitation of "bR_{605}" at 21 ± 1 °C. The delay times for observation are (a) −118, (b) −49, (c) −33, (d) 21, (e) 35, (f) 43, (g) 66, (h) 125, and (i) 217 ps. Twelve to sixteen pairs of excitation and nonexcitation data were averaged. The downward spikes in spectra d–i are due to the scattered excitation light pulse.

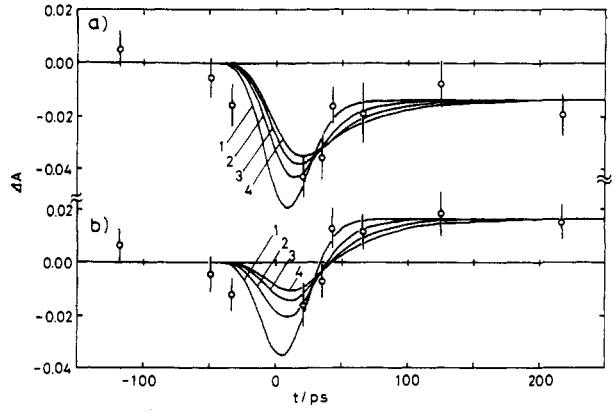

FIGURE 2: Picosecond kinetics of transient absorption of "bR_{605}" following the 630-nm excitation at 21 ± 1 °C. Absorbance changes were averaged over (a) 570–620- and (b) 640–690-nm regions. Solid curves 1, 2, 3, and 4 were obtained by convolution of the excitation pulse (20-ps fwhm), probe pulse (30-ps fwhm), and exponential decay functions of 10, 20, 30, and 40 ps, respectively.

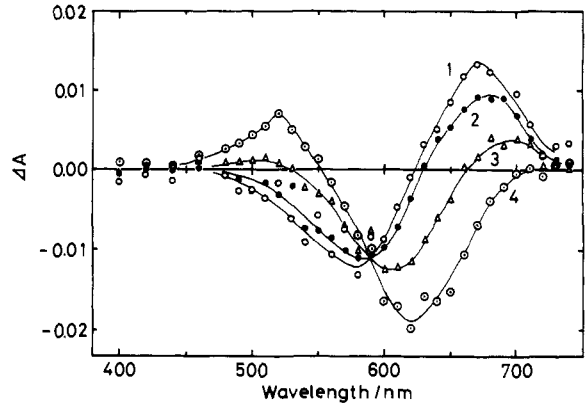

FIGURE 3: Nanosecond time-resolved difference spectra following 630-nm excitation of "bR_{605}" at 21 ± 1 °C. Curves 1, 2, 3, and 4 show the transient spectra 150 ± 50 ns, 500 ± 100 ns, 1.5 ± 0.25 μs, and 7 ± 0.5 μs after excitation, respectively. Data obtained by 16 laser shots were averaged for each observed wavelength.

decay functions of 10, 20, 30, and 40 ps, respectively, with the fitting parameter of the amplitude of absorbance change, where the pulse widths of the probe and excitation lights were set at 20 and 30 ps (fwhm), respectively. The time constant was obtained at 10 ps for both the experimental data in Figure 2 by the least-squares best fitting method. The upper limit of the time constant is 30 ps. The time constant (τ) was also estimated by $\tau/\Delta t = \Delta A_{obsd}/\Delta A$, where Δt is the time resolution of the picosecond apparatus (36 ps) and ΔA is the absorbance change that would be observed if the resolution time were much shorter than the lifetime of the precursor of K_{acid}. The observed absorbance change (ΔA_{obsd}) is −0.045 at 600 nm. The absorbance change (ΔA) due to the 73 ± 7% bleaching of the sample is calculated to be −0.87 ± 0.07 on the assumption that there is no absorption due to transient species in the bleaching spectral region. If there is transient absorption, the value of $|\Delta A|$ would be smaller than 0.87. The lower limit of the time constant was therefore estimated to be 2 ps.

Figures 1 and 2 show that there is a precursor of K_{acid}, which has absorption in the 500–520-nm region. It appears within 21 ps after excitation (Figure 1d) and disappears at 43 ps (Figure 1f). Matveetz et al. (1985) also observed a hypsochromically shifted transient absorption (410–510 nm) 0.5 ps after excitation of bacteriorhodopsin in neutral pH suspension and assigned it to the $S_n \leftarrow S_1$ transition. Therefore, the precursor of K_{acid} is attributed to S_1 in $bR_{605}^{all\text{-}tr}$.

Nanosecond Time-Resolved Spectroscopy with 630-nm Excitation Light. Figure 3 exhibits the time-resolved difference spectra observed between 150 ns and 7 μs after the 630-nm excitation. The transient spectra 150 ns (curve 1) and 217 ps (Figure 1i) after excitation resemble each other (Kobayashi et al., 1983). The time dependence of the difference spectra shows that an absorption around 670 nm due to K_{acid} decays within 7 μs and an absorption around 520 nm appears (curve 4). The spectral change is due to the formation of the species blue-shifted from $bR_{605}^{all\text{-}tr}$.

Figure 4a–h shows the kinetics of the transient absorbance change between 0 and 9 μs at several wavelengths. The time dependence of ΔA at all observed wavelengths and the time-resolved difference spectra between 0 and 9 μs are summarized as follows: (i) ΔA decreases with time in wavelength regions

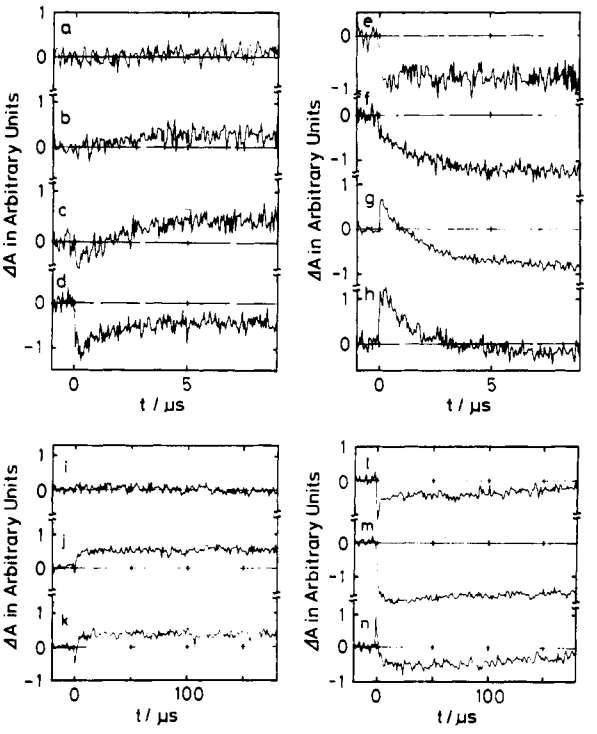

FIGURE 4: Kinetics of transient absorbance change following 630-nm excitation of "bR_{605}" at 21 ± 1 °C. The monitoring wavelengths are (a) 400, (b) 480, (c) 530, (d) 570, (e) 590, (f) 610, (g) 650, (h) 690, (i) 420, (j) 500, (k) 540, (l) 570, (m) 610, and (n) 680 nm. Sixteen and thirty-two shots were averaged for curves a–f and h and for curve g, respectively. Eight laser shots were averaged for curves i–n. Time resolutions are 50 and 500 ns for curves a–h and i–n, respectively.

longer than 600 nm. (ii) ΔA increases with time in wavelength regions between about 450 and 580 nm. (iii) An isosbestic point lies between 580 and 590 nm. (iv) $|\Delta A|$ at all observed wavelengths decays exponentially with the same time constant ($\tau_{1/e}$) of 1.5 ± 0.3 μs.

The time constant for the conversion process of K_{acid} → the blue-shifted species in the acidified sample is very close to that for the KL → L conversion in neutral-pH suspension (1.3 ± 0.3 μs; Kobayashi et al., 1983). The change in the difference spectrum observed between 150 ns and 7 μs after excitation is attributed to the conversion from K_{acid} to the acidic for of L (L_{acid}).

Figure 4i–n shows the kinetics of the transient absorption up to 180 μs after the 630-nm excitation. The initial spikes in Figure 4j–l,n are due to K_{acid}. Figure 4j,k shows the lifetime of L_{acid} is much longer than 180 μs.

Nanosecond Time-Resolved Spectroscopy with 532-nm Excitation Light. All components of "bR_{605}" ($bR_{605}^{all\text{-}tr}$, $bR_{605}^{13\text{-}cis}$, and a small amount of bR_{568}) are excited by the 532-nm light. Figure 5 shows the time-resolved difference spectra 100 ns, 7 μs, and 90 μs after 532-nm excitation. The transient absorption spectrum at 100 ns is different from those of the 630-nm excitation at 150 ns (Figure 3) because of the formation of K_{acid}, KL, and a photoproduct of $bR_{605}^{13\text{-}cis}$. The absorption in the 610–700-nm region (curve 1 in Figure 5) decays with a time constant of 1.3 ± 0.1 μs, which agrees with the recovery of the absorption in the 460–500-nm region (1.3 ± 0.2 μs). These time constants are close to those of the 630-nm excitation experiments (1.5 ± 0.3 μs). The time constants for the K_{acid} → L_{acid} and KL → L conversions are the same (1.3 ± 0.2 μs). Therefore, the K_{acid} → L_{acid} and KL → L conversions are insensitive to pH. The lifetime of the photoproduct of $bR_{605}^{13\text{-}cis}$ is much longer than 9 μs, as shown by the 266-nm excitation experiment (see below).

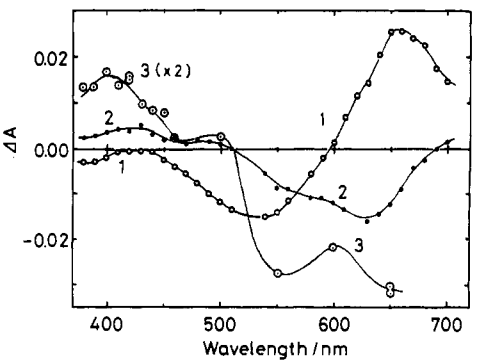

FIGURE 5: Nanosecond time-resolved difference spectra following 532-nm excitation of "bR_{605}" at 21 ± 1 °C. Curves 1, 2, and 3 show transient spectra 100 ns, 7 μs, and 90 μs after excitation, respectively. Thirty-two laser shots were averaged for each observed wavelength.

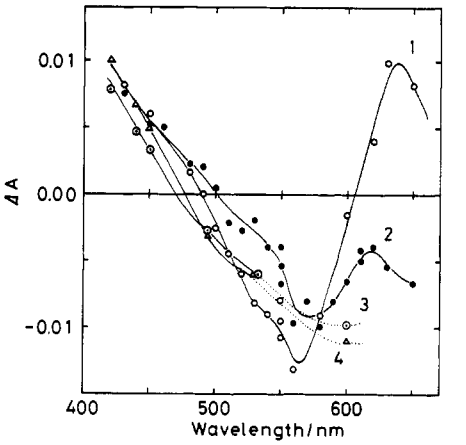

FIGURE 6: Nanosecond time-resolved difference spectra following 266-nm excitation of "bR_{605}" at 21 ± 1 °C. Curves 1, 2, 3, and 4 show transient spectra 100 ns, 7 μs, 200 μs, and 1.8 ms after excitation, respectively. Sixty-four laser shots were averaged for each observed wavelength.

The difference spectrum 90 μs after 532-nm excitation has a positive ΔA in the 380–420-nm region (curve 3 in Figure 5) due to M, which is absent after the 630-nm excitation (Figure 4i). M could be formed by 532-nm excitation of a small amount of the neutral form bR_{568} in the low-pH sample. The lifetime (32 ± 10 μs) of the neutral form L in low-pH suspension measured at 550 nm agrees with the formation time of M (33 ± 8 μs) measured at 415 nm. The time constant for the L → M conversion in low-pH suspension is about 3 times shorter than in neutral pH suspensions (102 ± 12 μs; Kobayashi et al., 1983).

Nanosecond Time-Resolved Spectroscopy with 266-nm Excitation Light. The excited bR_{568} in sample "bR_{605}" is negligibly small (Table I). Figure 6 shows the nanosecond time-resolved difference spectra of "bR_{605}" following the excitation by a 5-ns pulse at 266 nm. An absorbance change maximum (630–640 nm) and an isosbestic point (610 nm) at 100-ns delay time are shifted to shorter wavelength from those in Figure 3 (curve 1; 150 ns after excitation). The shift could be due to an intermediate in the photocycle of $bR_{605}^{13\text{-}cis}$. The time constants for the decay at 650 nm and the rise at 500 nm are both 1.2 ± 0.2 μs. The intermediate in the photocycle of $bR_{605}^{13\text{-}cis}$ (C_{acid}) does not decay up to 7 μs (absorbance change maximum around 610–620 nm shown by curve 2 in Figure 6).

An intense absorption was observed at wavelengths shorter than 450 nm just after excitation (<5 ns). This was not observed under 532- or 630-nm pulse irradiation. The decay time constants for the transient absorbance changes at 420

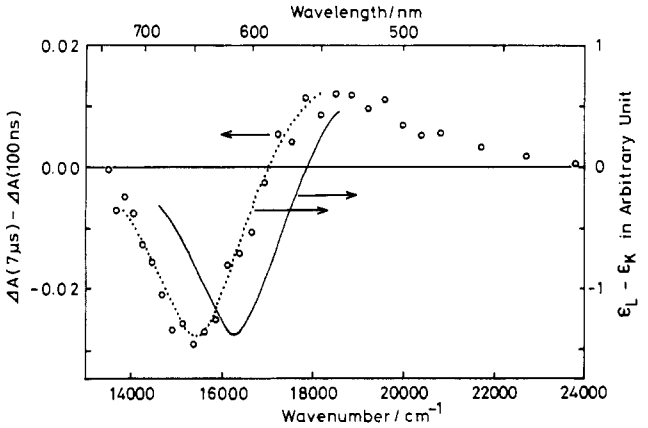

FIGURE 7: L-minus-K difference spectra. Open circles are differences in absorbance change between $\Delta A(7\ \mu s)$ and $\Delta A(100\ ns)$ following 630-nm excitation at 21 ± 1 °C. The solid line is an L-minus-K difference absorption spectrum at 18 °C (Shichida et al., 1983). The dotted line is a spectrum of solid line 870 cm^{-1} shifted to the lower wavenumber.

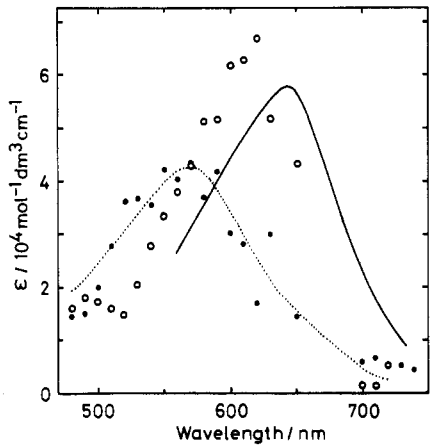

FIGURE 8: Absorption spectra of $bR_{605}^{all\text{-}tr}$ (open circles), $bR_{605}^{13\text{-}cis}$ (solid circles), K_{acid} (solid curve), and L_{acid} (dotted curve) at 21 ± 1 °C.

and 600 nm are 6 ± 1 ms. An unknown transient, T_{420}, with an absorption around 420 nm evidently changes into $bR_{605}^{all\text{-}tr}$ and/or $bR_{605}^{13\text{-}cis}$ with a time constant of 6 ± 1 ms. We estimated that time constant for the bleaching recovery at 620 nm to be 15 ± 5 ms from the data of Mowery et al. (1979). This is longer than the lifetime of T_{420}. Therefore, T_{420} is an intermediate in a new photocycle driven by UV light.

Intermediates K_{acid} and L_{acid} in the Photocycle of $bR_{605}^{all\text{-}tr}$. Open circles in Figure 7 show the difference in absorbance change, $\Delta(\Delta A)^{630ex}$, between $\Delta A(7\ \mu s)$ and $\Delta A(100\ ns)$ of "bR_{605}" induced by 630-nm excitation. The solid line in Figure 7 shows the L-minus-K difference spectrum of bacteriorhodopsin in neutral-pH suspension at room temperature (Shichida et al., 1983). These two difference spectra coincide with each other if one is shifted by 870 cm^{-1}. The spectra of K_{acid} and L_{acid} at room temperature are therefore assumed to be equal to the spectra of K and L shifted by 870 cm^{-1} to lower wavenumber. The molar extinction coefficients of K_{acid} and L_{acid} at their peaks were assumed to be equal to those of K and L, respectively. The absorption spectra with the assumed extinction coefficients of K_{acid} (ϵ^{AK}) and L_{acid} (ϵ^{AL}) are shown in Figure 8. The concentration of K_{acid} formed by 630-nm excitation and the quantum yield were estimated to be 2.6 × 10^{-6} mol dm^{-3} and 0.09 ± 0.01, respectively, with the use of the extinction coefficients.

The difference in absorbance change, $\Delta(\Delta A)^{532ex}$, between $\Delta A(7\ \mu s)$ and $\Delta A(100\ ns)$ of "bR_{605}" induced by 532-nm excitation (data not shown) differs from $\Delta(\Delta A)^{630ex}$ (open circles in Figure 7). The spectrum of $\Delta(\Delta A)^{532ex}$ is given by a superposition of the L_{acid}-minus-K_{acid} difference spectrum and L-minus-KL difference spectrum:

$$\Delta(\Delta A)^{532ex} = (\epsilon^{AL} - \epsilon^{AK})C_{AK}^{532ex}l + (\epsilon^{L} - \epsilon^{KL})C_{KL}^{532ex}l \qquad (1)$$

where ϵ^{AL}, ϵ^{AK}, ϵ^{L}, and ϵ^{KL} are the molar extinction coefficients of K_{acid}, L_{acid}, L, and KL, respectively, at room temperature. The concentrations of K_{acid} and KL (C_{AK}^{532ex} and C_{KL}^{532ex}, respectively) were found to be 3.7 × 10^{-6} and 1.5 × 10^{-6} mol dm^{-3}, respectively, by the least-squares best fitting method.

The spectrum of $\Delta(\Delta A)^{266ex}$ between $\Delta A(7\ \mu s)$ and $\Delta A(100$ ns) induced by 266-nm excitation of "bR_{605}" is similar to the open circles in Figure 7. The formations of KL and L were not clearly found because the absorbance change induced by 266-nm excitation (Figure 6) is smaller than that induced by 532-nm excitation (Figure 5). Observed temporal changes in the 10 ns to 9 μs time region are attributed to the $K_{acid} \rightarrow L_{acid}$ conversion. The concentration of the intermediate in $bR_{605}^{13\text{-}cis}$ photocycle is apparently constant in the 10 ns to 9 μs time region.

Absorption Spectra of $bR_{605}^{all\text{-}tr}$ and $bR_{605}^{13\text{-}cis}$. The molar extinction coefficients of $bR_{605}^{all\text{-}tr}$ (ϵ^{T}) and $bR_{605}^{13\text{-}cis}$ (ϵ^{C}) are shown in Figure 8. They were obtained with the method described in the Appendix. The absorption spectrum of $bR_{605}^{all\text{-}tr}$ (λ_{max} = 610–620 nm) agrees with the fluorescence excitation spectrum of bacteriorhodopsin at pH 2.6 (λ_{max} = 613–614 nm; Kouyama et al., 1985). The absorption spectrum of $bR_{605}^{13\text{-}cis}$ resembles that of L_{acid} and, its peak wavelength (550–570 nm) is shorter than that of $bR_{605}^{all\text{-}tr}$.

Intermediate C_{acid} in the Photocycle of $bR_{605}^{13\text{-}cis}$. A difference absorption spectrum, $\Delta A - \Delta A(bR_{605}^{all\text{-}tr})$, shown in Figure 9 is obtained by correction for the absorbance change, $\Delta A(bR_{605}^{all\text{-}tr})$, due to the photochemical process of $bR_{605}^{all\text{-}tr}$ by using the following equation with excitation wavelength λ = 266 nm:

$$\begin{aligned} \Delta A(bR_{605}^{all\text{-}tr}) &= (\epsilon^{AK} - \epsilon^{T})C_{AK}^{\lambda ex}l \quad \text{at 100 ns} \\ \Delta A(bR_{605}^{all\text{-}tr}) &= (\epsilon^{AL} - \epsilon^{T})C_{AK}^{\lambda ex}l \quad \text{at 7 } \mu s \end{aligned} \qquad (2)$$

Here ϵ^{T} is the molar extinction coefficient of $bR_{605}^{all\text{-}tr}$. The concentration ($C_{AK}^{\lambda ex}$) of K_{acid} generated by the excitation at λ = 266 nm was determined to be 1.3 × 10^{-6} mol dm^{-3} with

$$C_{AK}^{\lambda ex} = \Delta(\Delta A)^{\lambda ex}/(\epsilon^{AL} - \epsilon^{AK})l \qquad (3)$$

The spectral shape in the 580–650-nm wavelength region resembles those measured by Kalisky et al. (1977) and by Iwasa et al. (1981). A photoproduct of $bR_{605}^{13\text{-}cis}$ (C_{acid}) corresponds to ^{610}C (Dencher et al., 1977; Kalisky et al., 1977)

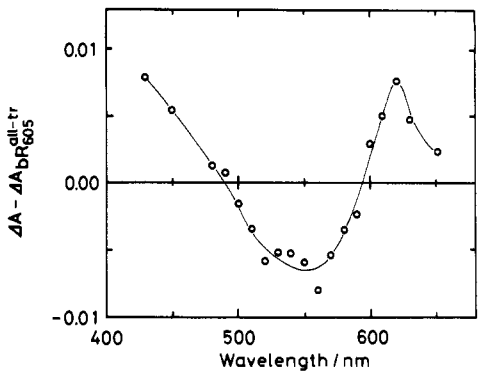

FIGURE 9: Difference spectrum $\Delta A^{266ex} - \Delta A^{all\text{-}tr}$ at 21 ± 1 °C. The spectra $\Delta A^{266ex}(100\ ns) - C_{AK}^{266ex}(\epsilon^{AK} - \epsilon^{T})l$ and $\Delta A^{266ex}(7\ \mu s) - C_{AL}^{266ex}(\epsilon^{AL} - \epsilon^{T})l$ were averaged.

Scheme I

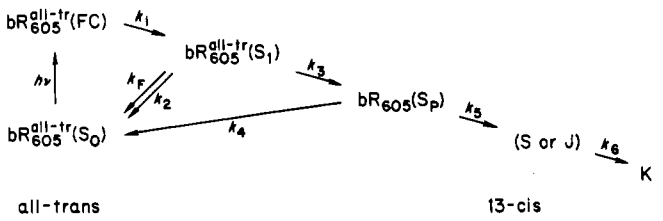

and Batho-bR[13] (Iwasa et al., 1981) in neutral-pH suspension. The formation yield of C_{alcd} was found to be nearly equal to that of ^{610}C obtained by the reported absorbance change (Kalisky et al., 1977). The spectroscopic and kinetic properties of the 13-cis pigment are less sensitive to pH than those of the all-trans pigment.

Discussion

The sample solution of the acidified bacteriorhodopsin "bR_{605}" is a mixture of $bR_{605}^{all\text{-}tr}$ (57%), $bR_{605}^{13\text{-}cis}$ (40%), and bR_{568} (3%). Absorption spectra of $bR_{605}^{all\text{-}tr}$ and $bR_{605}^{13\text{-}cis}$ are shown in Figure 8. The 630-nm light drives mainly the photochemical cycle of $bR_{605}^{all\text{-}tr}$. The 532- and 266-nm pulses drive the photochemical cycles of $bR_{605}^{all\text{-}tr}$, $bR_{605}^{13\text{-}cis}$, and bR_{568} (Table I).

Picosecond Phenomena. In a preceding paper we described the effect of pH on the L → M process in the microsecond region (Kobayashi et al., 1983). The newly found pH effects on picosecond processes are the following: (i) the singlet (S_1) lifetime of $bR_{605}^{all\text{-}tr}$ (2–30 ps) is longer than that of bR_{568} [0.7 ± 0.1 ps, Downer et al. (1984); 0.7 ± 0.3 ps, Matveetz et al. (1985); 430 ± 50 fs, Nuss et al. (1985)] and (ii) the quantum yield of K_{acid} (0.09 ± 0.01) is smaller than that of K [0.30 ± 0.03, Becher and Ebrey (1977)]. Kouyama et al. (1985) reported that the fluorescence intensity of bacteriorhodopsin at pH 2 was about 13 times stronger than at pH 7. The larger fluorescence yield is due to the decrease in the nonradiative decay rate at low pH. $bR_{605}^{all\text{-}tr}$ may be fluorescent more than $bR_{605}^{13\text{-}cis}$ because the spectroscopic and kinetic properties of the all-trans pigment are sensitive to pH more than those of the 13-cis pigment; i.e., (i) the pH-dependent shift in the absorption maximum is larger in the all-trans pigment (40–50 nm) than in the 13-cis pigment (20–30 nm), and (ii) the yield of K_{acid} (0.09) is smaller than that of KL (0.3) though the yields of C_{acid} and ^{610}C are nearly equal to each other. The singlet lifetime of $bR_{605}^{all\text{-}tr}$ is estimated to be 6.7–17 ps from the reported singlet lifetime of bR_{568} (0.38–1.0 ps) and the fluorescence quantum yield [$(4.5 \pm 0.2) \times 10^{-3}$] on the assumption that the fluorescence yield of $bR_{605}^{13\text{-}cis}$ is equal to that of bR_{548} [$(0.7\text{–}1.2) \times 10^{-4}$, Kouyama et al., (1985)]. The singlet lifetime of $bR_{605}^{all\text{-}tr}$ obtained in the present study (2–30 ps) is consistent with this estimate.

Braiman and Mathies (1982) reported that the K intermediate has a 13-cis chromophore. By analogy with photoisomerization of stilbene there may be a phantom excited state (Hammond et al., 1964) with a twisted 13–14 carbon–carbon bond. $bR_{605}^{all\text{-}tr}$ in S_1 could relax rapidly to the phantom excited singlet state (S_P). The reaction sequence in the picosecond time domain is give in Scheme I, in which $bR_{605}^{all\text{-}tr}(FC)$ represents $bR_{605}^{all\text{-}tr}$ in the Franck–Condon state. The increase in the fluorescence yield and the decrease in the formation yield of K with the decrease in pH are attributed to a decrease in k_3, and possibly also in $k_5/(k_4 + k_5)$. Intermediate S (or J) was not detected in the photolysis of bR_{605}. The formation time of K_{acid} agrees with the singlet lifetime determined from the kinetics of the bleaching recovery in the 560–620-nm spectral region. Further study must be performed to clarify whether or not the acidic form of S (or J) exists in the bleaching process of "bR_{605}".

Nanosecond to Microsecond Phenomena. The formation of K_{acid} is observed in time-resolved experiments at room temperature (Figures 1–6). Maeda et al. (1981) reported that three intermediates, one red-shifted and two blue-shifted, are formed with >610-nm light irradiation of acidified bacteriorhodopsin at three different temperatures: −190, −72, and 0 °C. The final species formed at 0 °C was assigned to bR_{495}, which has a 9-cis chromophore (Maeda et al., 1980). The difference absorption spectrum at −72 °C is different from that at 0 °C and resembles the spectrum 7 μs after 630-nm excitation at 21 ± 1 °C in the present study (curve 4 in Figure 3). The blue-shifted species at −72 °C and the red-shifted species formed at −190 °C were assigned to L_{acid} and K_{acid}, respectively. The shift of the isosbestic point from 625 ± 5 nm at 21 ± 1 °C to 610 nm at −190 °C may be due either to larger formation efficiency of C_{acid} or to a change in the molar extinction coefficient of K_{acid} at low temperature.

The time constant and quantum yield for the $K_{acid} \rightarrow L_{acid}$ conversion are the same as those for KL → L in neutral-pH suspension. On the other hand the L → M process is highly sensitive to pH. Presumably, the proton of the Schiff base in L_{acid} cannot be released because a relevant proton-acceptor site has already been protonated. It must be noted that in low-pH suspension there is a neutral form L different from L_{acid}. The efficiency $\Phi_{L\rightarrow M}$ (the concentration ratio of M and L, C_M/C_L) was determined to be 0.41 by using the value of C_M obtained from the absorbance change at 410 nm 100 μs after excitation. The low efficiency and the short conversion time (32 ± 10 μs) are due to opening of a new decay channel from L to $bR_{605}^{all\text{-}tr}$ and/or $bR_{605}^{13\text{-}cis}$ (X):

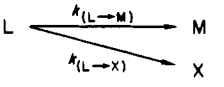

The rate constants $k_{L\rightarrow M}$ and $k_{L\rightarrow X}$ are obtained to be 1.3×10^4 and 1.8×10^4 s^{-1}, respectively.

L_{acid} and $bR_{605}^{13\text{-}cis}$ have similar absorption spectra. If L_{acid} is actually $bR_{605}^{13\text{-}cis}$, then the $L_{acid} \rightarrow bR_{605}^{all\text{-}tr}$ conversion process could correspond to the dark adaptation of the acidified bR. The recovery time of $bR_{605}^{all\text{-}tr}$ following 588-nm excitation of bR_{605} is 15 ± 5 ms (Mowery et al., 1979). Thus the the fast dark adaptation of bR_{605} can be explained.

Let us consider the photocycle of $bR_{605}^{13\text{-}cis}$. C_{acid} may be converted to bR_{605} on the analogy of the $^{610}C \rightarrow bR_{568}$ conversion in neutral-pH suspension. Figures 8 and 9 show that the absorption spectrum of C_{acid} resembles that of $bR_{605}^{all\text{-}tr}$, and therefore C_{acid} may actually be $bR_{605}^{all\text{-}tr}$.

A new intermediate, T_{420}, appears in the <450 nm wavelength region immediately after 266-nm excitation (<5 ns). T_{420} is not formed by 532- or 630-nm light, and it cannot be an excited state because of its long lifetime (6 ± 1 ms). Kalisky et al. (1977) claimed that M is formed by a multiphoton process with visible light. T_{420} may be M which is formed by the excitation of $bR_{605}^{13\text{-}cis}$ with 266-nm light be a single-photon process.

In "bR_{605}" the early stages of the photochemical cycles for $bR_{605}^{all\text{-}tr}$, $bR_{605}^{13\text{-}cis}$, and bR_{568} are independently initiated by light. The obseved transient difference spectra can be explained in terms of the superposition of changes caused in the three photochemical cycles shown in Figure 10.

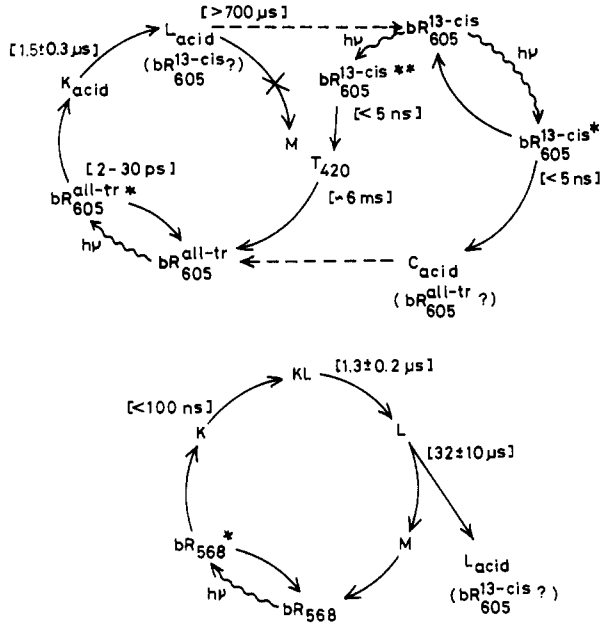

FIGURE 10: Photochemical cycles of $bR^{all\text{-}tr}_{605}$, $bR^{13\text{-}cis}_{605}$, and bR_{568} in low-pH suspension at 21 ± 1 °C. C_{acid} and L_{acid} may actually be $bR^{all\text{-}tr}_{605}$ and $bR^{13\text{-}cis}_{605}$, respectively. The lifetimes of intermediates are shown in brackets. The symbols * and ** show the lowest and the higher excited states, respectively.

ACKNOWLEDGMENTS

We thank Dr. Hisao Uchiki and Masayuki Yoshizawa, The University of Tokyo, for their assistance in data analysis and Keiko Nakajima, Institute of Physical and Chemical Research (IPCR), for her help in sample preparation. We also thank Drs. Tsutomu Kouyama and Kazuhiko Kinosita, Jr., IPCR, for their discussion.

APPENDIX

The molar extinction coefficients of $bR^{all\text{-}tr}_{605}$ (ϵ^T) and $bR^{13\text{-}cis}_{605}$ (ϵ^C) and the molar fraction of bR_{568} (f_p) were determined from

$$\Delta A(100\text{ ns})^\lambda = C^{\lambda ex}_{AK}(\epsilon^{AK} - \epsilon^T)l + C^{\lambda ex}_{AC}(\epsilon^{AC} - \epsilon^C)l + C^{\lambda ex}_{KL}(\epsilon^{KL} - \epsilon^P)l \quad (4)$$

$$\Delta A(7\ \mu s)^\lambda = C^{\lambda ex}_{AL}(\epsilon^{AL} - \epsilon^T)l + C^{\lambda ex}_{AC}(\epsilon^{AC} - \epsilon^C)l + C^{\lambda ex}_{L}(\epsilon^{L} - \epsilon^P)l \quad (5)$$

$$C^{\lambda ex}_{AK}:C^{\lambda ex}_{AC}:C^{\lambda ex}_{KL} = F_T(\lambda)\Phi_{AK}:F_C(\lambda)\Phi_{AC}:F_P(\lambda)\Phi_{KL} \quad (6)$$

$$\epsilon^B = f_T\epsilon^T + f_C\epsilon^C + f_P\epsilon^P \quad (7)$$

Here λ and l represent the excitation wavelength (630, 532, or 266 nm) and the light path length (0.3 cm), respectively. The concentrations of K_{acid} (C_{KA}) and KL (C_{KL}) were obtained by eq 1 and 3. The quantum yields for the formations of K_{acid} (Φ_{AK}) and KL (Φ_{KL}) are 0.09 (this work) and 0.3 (Becher & Ebrey, 1977), respectively. The molar fraction of component i (=T, C, and P) is denoted by f_i, where $f_T + f_P$ and f_C are known to be 0.6 and 0.4, respectively (Mowery et al., 1979; Maeda et al., 1980; Smith et al., 1985). The fraction of photon number absorbed by component i is denoted by F_i [$=f_i\epsilon^i(\lambda)/\sum_i f_i\epsilon_i(\lambda)$]. The molar extinction coefficient of "bR_{605}" (ϵ^B) has been determined (see Materials and Methods).

REFERENCES

Applebury, M. L., Peters, K. S., & Rentzepis, P. M. (1978) *Biophys. J. 23*, 375–382.

Becher, B., & Cassim, J. Y. (1976) *Biophys. J. 16*, 1183–1200.

Becher, B., & Ebrey, T. G. (1977) *Biophys. J. 17*, 185–191.

Braiman, M., & Mathies, R. (1982) *Proc. Natl. Acad. Sci. U.S.A. 79*, 403–407.

Dencher, N. A., Rafferty, C. N., & Sperling, W. (1976) *Ber. Kernforschungsanlage Juelich Juel-1374*, 1–42.

Downer, M. C., Islam, M., Shank, C. V., Harootunian, A., & Lewis, A. (1984) in *Picosecond Phenomena IV* (Auston, D. H., & Eisenthal, K. B., Eds.) pp 500–502, Springer-Verlag, Berlin.

Fischer, U. C., Towner, P., & Oesterhelt, D. (1981) *Photochem. Photobiol. 33*, 529–537.

Hammond, G. S., Saltiel, J., Lamola, A. A., Turro, N. J., Bradshaw, J. S., Cowan, D. O., Counsell, R. C., Vogt, V., & Dalton, C. (1964) *J. Am. Chem. Soc. 86*, 3197–3217.

Honig, B. (1978) *Annu. Rev. Phys. Chem. 29*, 31–57.

Ippen, E. P., Shank, C. V., Lewis, A., & Marcus, M. A. (1978) *Science (Washington, D.C.) 200*, 1279–1281.

Iwai, J., Ikeuchi, M., Inoue, Y., & Kobayashi, T. (1984) in *Protochlorophyllide Reduction and Greening* (Sironval, C., & Brouers, M., Eds.) pp 99–112, Nijhoff/Junk Publishers, The Hague.

Iwasa, T., Tokunaga, F., & Yoshizawa, T. (1980) *Biophys. Struct. Mech. 6*, 253–270.

Iwasa, T., Tokunaga, F., & Yoshizawa, T. (1981) *Photochem. Photobiol. 33*, 539–545.

Kalisky, O., Goldschmidt, C. R., & Ottolenghi, M. (1977) *Biophys. J. 19*, 185–189.

Kaufmann, K. J., Rentzepis, P. M., Stoeckenius, W., & Lewis, A. (1976) *Biochem. Biophys. Res. Commun. 68*, 1109–1115.

Kimura, Y., Ikegami, A., & Stoeckenius, W. (1984) *Photochem. Photobiol. 40*, 641–646.

Kobayashi, T., Ohtani, H., Iwai, J., Ikegami, A., & Uchiki, H. (1983) *FEBS Lett. 162*, 197–200.

Kobayashi, T., Ohtani, H., Iwai, J., & Ikegami, A. (1984a) in *Ultrafast Phenomena IV* (Auston, D. H., & Eisenthal, K. B., Eds.) pp 481–483, Springer-Verlag, Berlin.

Kobayashi, T., Ohtani, H., Iwai, J., & Ikegami, A. (1984b) in *Proceedings of the International Symposium on Fast Reactions in Biological Systems*, pp 90–91, Kyoto, Japan.

Kouyama, T., Kinosita, K., Jr., & Ikegami, A. (1985) *Biophys. J. 47*, 43–54.

Kugel, R., Svirmickas, A., Katz, J. J., & Hindman, J. C. (1977) *Opt. Commun. 23*, 189–193.

Kung, M. C., DeVault, D., Hess, B., & Oesterhelt, D. (1975) *Biophys. J. 15*, 907–911.

Lozier, R. H., Bogomolni, R. A., & Stoeckenius, W. (1975) *Biophys. J. 15*, 955–962.

Maeda, A., Iwasa, T., & Yoshizawa, T. (1980) *Biochemistry 19*, 3825–3831.

Maeda, A., Iwasa, T., & Yoshizawa, T. (1981) *Photochem. Photobiol. 33*, 559–565.

Matveetz, Yu. A., Chekalin, S. V., & Sharkov, A. V. (1985) *J. Opt. Soc. Am. B: Opt. Phys. 2*, 634–639.

Mowery, P. C., Lozier, R. H., Chae, Q., Tseng, Y.-W., Taylor, M., & Stoeckenius, W. (1979) *Biochemistry 18*, 4100–4107.

Nuss, M. C., Zinth, W., Kaiser, W., Kolling, E., & Oesterhelt, D. (1985) *Chem. Phys. Lett. 117*, 1–7.

Oesterhelt, D., & Stoeckenius, W. (1971) *Nature (London), New Biol. 233*, 149–152.

Oesterhelt, D., & Stoeckenius, W. (1974) *Methods Enzymol. 31*, 667–678.

Ohno, T., Kato, S., & Lichtin, N. N. (1982) *Bull. Chem. Soc. Jpn. 55*, 2753–2759.

Ohtani, H., Kobayashi, T., Iwai, J., & Ikegami, A. (1984) in *Proceedings of the International Symposium on Fast Reactions in Biological Systems*, pp 100–101, Kyoto, Japan.

Rehorek, M., & Heyn, M. P. (1979) *Biochemistry 18*, 4977–4983.
Shichida, Y., Matuoka, S., Hidaka, Y., & Yoshizawa, T. (1983) *Biochim. Biophys. Acta 723*, 240–246.
Smith, S. O., & Mathies, R. A. (1985) *Biophys. J. 47*, 251–254.
Sperling, W., Carl, P., Rafferty, C. N., & Dencher, N. A. (1977) *Biophys. Struct. Mech. 3*, 79–94.
Stoeckenius, S., Lozier, R. H., & Bogomolni, R. A. (1979) *Biochim. Biophys. Acta 505*, 215–278.
Vincett, P. S., Voigt, E. M., & Reickhoff, K. E. (1971) *J. Chem. Phys. 55*, 4131–4140.

Transient Kinetics of Reduction of Blue Copper Proteins by Free Flavin and Flavodoxin Semiquinones†

G. Tollin,*,‡ T. E. Meyer,‡ G. Cheddar,‡ E. D. Getzoff,§ and M. A. Cusanovich‡

Department of Biochemistry, University of Arizona, Tucson, Arizona 85721, and Department of Molecular Biology, Scripps Clinic and Research Foundation, La Jolla, California 92037

Received October 25, 1985; Revised Manuscript Received February 5, 1986

ABSTRACT: Rate constants have been determined for the electron-transfer reactions between reduced free flavins and flavodoxin semiquinone and several blue copper proteins. Correlations between these values and redox potentials demonstrate that spinach plastocyanin, *Pseudomonas aeruginosa* azurin, *Alcaligenes* sp. azurin, and *Alcaligenes* sp. nitrite reductase have the same intrinsic reactivities toward free flavins, whereas stellacyanin is more reactive (3.3 times) and laccase considerably less reactive (~12 times). Electrostatic interactions between the negatively charged flavin mononucleotide (FMN) and the copper proteins show that the interaction site charges for laccase and nitrite reductase are opposite in sign to the net protein charge and that the signs and magnitudes of the charges are consistent with the known three-dimensional structures for plastocyanin and the azurins and with amino acid sequence homologies for stellacyanin. The results demonstrate that the apparent interaction site charge with flavodoxin is larger than that with FMN for plastocyanin, nitrite reductase, and stellacyanin but smaller for *Pseudomonas* azurin. This is interpreted in terms of a larger interaction domain for the flavodoxin reaction, which allows charged groups more distant from the actual electron-transfer site to become involved. The intrinsic reactivities of plastocyanin and azurin toward flavodoxin are the same, as was the case with FMN, but both stellacyanin and nitrite reductase are considerably less reactive than expected (approximately 2 orders of magnitude). This result suggests the involvement of steric factors with these latter two proteins which discriminate against large reactants such as flavodoxin.

The electron-transfer reactions and spectroscopic properties of the intensely blue copper proteins have been the focus of considerable research [for reviews, see Holwerda et al. (1976), Solomon et al. (1983), and Adman (1985)]. Most kinetic studies have utilized reactions with inorganic and small organic reductants and oxidants, although in some cases protein–protein interactions have been examined (Farver et al., 1982; Augustin et al., 1984; Takabe et al., 1984; Beoku-Betts et al., 1985). Both temperature (Sailasuta et al., 1979) and pH (Rosenberg et al., 1976) effects have been investigated. Ionic strength effects, which are known to be large in other systems, have also been studied to some extent [cf. Sisley et al. (1983)]. This previous work has led to the conclusions that electron-transfer rate constants are relatively insensitive to pH [cf. also Ugurbil and Mitra (1985)] and that the apparent charge at the electron-transfer site has the same sign as the overall protein charge at pH 7 [cf. Holwerda et al. (1976) and Sisley et al. (1983)], although one exception to this has been reported with stellacyanin (Cummins & Gray, 1977).

The most commonly used copper proteins for kinetic analysis have been plant plastocyanins, bacterial azurins, tree (*Rhus vernicifera*) laccase, and stellacyanin. All but laccase are simple, low molecular weight proteins containing a single copper atom. Amino acid sequences of azurin, plastocyanin, and stellacyanin indicate that they are homologous, although the sequences are difficult to align because of insertions and deletions (Boulter et al., 1977; Norris et al., 1983). The three-dimensional (3-D) structures of azurins (Adman et al., 1978; Norris et al., 1983) and plastocyanin (Colman et al., 1978; Guss & Freeman 1983) show that both proteins have very similar copper binding sites and that there is considerable conservation of β-type secondary structure and indicate where insertions and deletions are likely to have occurred. Laccase is a large oxidase that contains, in addition to the intensely blue or type 1 copper, a paramagnetic but otherwise spectrally invisible type 2 copper and a diamagnetic, UV-absorbing type 3 binuclear copper center. Previous kinetic studies have indicated that stellacyanin is significantly more reactive, and the type 1 copper center in laccase is considerably less reactive, than plastocyanin and azurin [cf. Holwerda et al. (1976)]. On

† Supported in part by grants from the National Institutes of Health (AM15057 to G.T. and GM21277 to M.A.C.).
* Author to whom correspondence should be addressed.
‡ University of Arizona.
§ Scripps Clinic and Research Foundation.

0006-2960/86/0425-3363$01.50/0